

Using Vertically Integrated Ocean Fields to Characterize Greenland Icebergs' Distribution and Lifetime

Juliana M. Marson, Paul G. Myers, Xianmin Hu, Julien Le Sommer

▶ **To cite this version:**

Juliana M. Marson, Paul G. Myers, Xianmin Hu, Julien Le Sommer. Using Vertically Integrated Ocean Fields to Characterize Greenland Icebergs' Distribution and Lifetime. Geophysical Research Letters, 2018, 45, pp.4208-4217. 10.1029/2018GL077676 . insu-03706508

HAL Id: insu-03706508

https://insu.hal.science/insu-03706508

Submitted on 28 Jun 2022

HAL is a multi-disciplinary open access archive for the deposit and dissemination of scientific research documents, whether they are published or not. The documents may come from teaching and research institutions in France or abroad, or from public or private research centers.

L'archive ouverte pluridisciplinaire **HAL**, est destinée au dépôt et à la diffusion de documents scientifiques de niveau recherche, publiés ou non, émanant des établissements d'enseignement et de recherche français ou étrangers, des laboratoires publics ou privés.

Copyright

Check for updates

AGU100 ADVANCING EARTH AND SPACE SCIENCE

Geophysical Research Letters

RESEARCH LETTER
10.1029/2018GL077676

Using Vertically Integrated Ocean Fields to Characterize Greenland Icebergs' Distribution and Lifetime

Juliana M. Marson[1], Paul G. Myers[1], Xianmin Hu[1,2], and Julien Le Sommer[3]

[1]Department of Earth and Atmospheric Sciences, University of Alberta, Edmonton, Alberta, Canada, [2]Now at Bedford Institute of Oceanography, Dartmouth, NS, Canada, [3]Université Grenoble-Alpes, CNRS, IRD, IGE, Grenoble, France

Abstract Icebergs represent approximately half of Greenland's yearly mass loss, having important implications for biological productivity, freshwater fluxes in the ocean, and navigation. This study applies an iceberg model that uses integrated ocean fields (from surface to iceberg keel) to simulate the drift and decay of Greenland icebergs. This version of iceberg model (*VERT*) is compared with a more widely adopted version (*SURF*) which only uses surface ocean fields in its equations. We show that icebergs in *VERT* tend to drift along the shelf break, while in *SURF* they concentrate along the coastline. Additionally, we show that Greenland's southeast coast is the source of ~60% of the icebergs that cross the interior of the Labrador Sea—a region that stages buoyancy-driven convection and is, therefore, sensitive to freshwater input.

Plain Language Summary Thousands of icebergs break off from Greenland every year, threatening navigation along North America's east coast. Since it is difficult to monitor individual icebergs, computer simulations are useful to help us understand their common pathways and, potentially, to predict when and from where icebergs come from. In this study, we use an improved iceberg model (one that uses the variations of ocean currents and temperature with depth to interact with icebergs) to simulate Greenland icebergs' distribution and their persistence in different regions of the North Atlantic. We show that this improved version better reproduces iceberg pathways observed in the past. Moreover, we find that icebergs breaking off from the southeast part of Greenland compose most icebergs reaching the middle of the Labrador Sea—a region where iceberg melt may affect ocean circulation and, consequently, heat distribution from tropics to poles. This means that an increasing volume of icebergs coming out of this particular region in a warmer world might have an effect back on the climate.

Key Points:
- In the vertically integrated version of NEMO-ICB most icebergs move along the shelf break within the main currents
- The lifetime of icebergs is reduced northeast of Greenland with the vertically integrated version of NEMO-ICB
- Around 60% of icebergs that reach the interior Labrador Sea calve from the southeast Greenland coast

Supporting Information:
- Supporting Information S1

Correspondence to:
J. M. Marson,
marson@ualberta.ca

Citation:
Marson, J. M., Myers, P. G., Hu, X., & Le Sommer, J. (2018). Using vertically integrated ocean fields to characterize Greenland icebergs' distribution and lifetime. *Geophysical Research Letters*, *45*, 4208–4217. https://doi.org/10.1029/2018GL077676

Received 23 FEB 2018
Accepted 14 APR 2018
Accepted article online 3 MAY 2018
Published online 11 MAY 2018

©2018. American Geophysical Union. All Rights Reserved.

1. Introduction

It is estimated that the Greenland Ice Sheet (GrIS) calves between 200 and 500 Gt of icebergs every year (Bamber et al., 2012; Bigg, 1999; Enderlin et al., 2014; Rignot et al., 2011), which corresponds to approximately half of the GrIS annual mass loss (e.g., Bamber et al., 2012; Enderlin et al., 2014). Icebergs are important because they are sources of nutrients (e.g., Duprat et al., 2016) and freshwater to the ocean. Compared to liquid runoff, icebergs carry the freshwater farther away from the coast (Martin & Adcroft, 2010) and so are more likely to be relevant for open ocean convection regions (e.g., the Labrador Sea), where freshwater can alter the density and rates at which deep waters are formed (Böning et al., 2016). Moreover, icebergs are a constant and yet, sometimes, unforeseen threat to ships and offshore structures in the North Atlantic. Given the recent warming trends and associated reducing sea ice cover (e.g., Stroeve et al., 2012), both shipping activity (Pizzolato et al., 2016) and calving (e.g., Straneo et al., 2013) are likely to increase in the Subarctic Atlantic and Canadian Arctic. Therefore, it is paramount to improve estimates such as the likelihood of icebergs occurring in a given region, their average lifetime, and their point of origin.

Observing the origin, dispersion, and disintegration of icebergs, however, is not easily done. The International Ice Patrol (IIP) and Canadian Ice Service (CIS) monitor icebergs that cross the ship lanes in the northwest Atlantic, but their coverage area is limited to aircraft range and ship tracks. Additionally, the deployment of instruments to monitor position and melting rate is limited to a few icebergs. Altimeters and radars are also useful to infer about the general distribution of icebergs, but those are limited in regions covered by thick sea ice (e.g., Tournadre et al., 2008; Wesche & Dierking, 2012, 2015). This is where modeling icebergs becomes particularly useful. Bigg et al. (1996, 1997) described an iceberg model whose goal is to simulate the overall

distribution of relatively small icebergs. This original version of the model, which uses only the surface ocean fields to calculate the drift and disintegration of icebergs, was further improved by Gladstone et al. (2001) and Martin and Adcroft (2010). Marsh et al. (2015) introduced the latter version into the Nucleus for European Modelling of the Ocean (NEMO) and suggested modifying the code in order to take into consideration the vertically integrated (from surface to iceberg keel) ocean fields to move and melt the icebergs. These changes were implemented by Merino et al. (2016), who then applied this vertically integrated version of the iceberg model to the Southern Ocean. Until now, this updated version of the iceberg model has not been applied to the North Atlantic.

To address the mentioned concerns, we (1) use the Merino et al. (2016) vertically integrated version of the iceberg model coupled with NEMO v3.4 to study the distribution and lifetime of icebergs originating from Greenland, (2) compare the results with the ones obtained with the "surface version" of the iceberg model, and (3) determine the patterns of iceberg distribution according to the sector of Greenland's coast they calved from.

2. Data and Simulation Details

The simulation was carried out with the NEMO v3.4 (Madec & the NEMO team, 2008) model coupled with the Louvain-la-Neuve Sea Ice Model (LIM2; Bouillon et al., 2009; Fichefet & Morales Maqueda, 1997). Detailed model parameters and setup was documented in Dukhovskoy et al. (2016). The domain covers the Arctic and Northern Hemisphere Atlantic (the ANHA configuration, http://knossos.eas.ualberta.ca/xianmin/anha/index.html), with open boundaries at 20° S in the Atlantic Ocean and at the Bering Strait, a horizontal resolution of 1/4° (ANHA4) and 50 vertical levels. The boundary and initial conditions are provided by GLORYS2v3 (Masina et al., 2015), and the hourly atmospheric forcing fields are supplied by the Canadian Meteorological Centre's global deterministic prediction system reforecasts (CGRF; Smith et al., 2014) from 2002 to 2015 at a spatial resolution of 33 km.

Two versions of the iceberg model (briefly described in Text S1 in the supporting information) were used in this study. The first one, used in the simulation we call *SURF*, follows the equations presented by Martin and Adcroft (2010; based on the original work of Bigg et al., 1997) and was implemented in NEMO v3.5 (NEMO-ICB) by Marsh et al. (2015). This version uses only surface ocean fields in the momentum and mass balance equations, and no grounding mechanism is present. The second version, implemented and described by Merino et al. (2016), uses vertically integrated ocean fields to move and melt icebergs. When integrating velocities along the iceberg draft in regions shallower than this draft, the iceberg speed is reduced which works as a grounding mechanism (equation (5) in Text S1). We used this version in the simulation we call *VERT*. In both versions of the model, the impact of sea ice on iceberg dynamics is only represented by the sea ice drag term in the momentum equation. There is no sea ice locking of icebergs, even when the sea ice pack is compact.

The iceberg model was seeded with 54% of the total mass loss from numerous marine-terminating glaciers in GrIS (Figure 1) estimated by an ice sheet mass balance model (Bamber et al., 2012) from 2002 to 2010. Calving rates vary monthly (peaking during summer) and interannually, but rates from 2010 were repeated for the years 2011 to 2015—which is a reasonable approximation, since solid discharge has not changed significantly since 2010 (Bamber et al., 2018). The percentage of total mass loss attributed to calving was calculated based on the averages of solid and liquid discharge presented by Bamber et al. (2012).

The International Ice Patrol (IIP) data (International Ice Patrol, 1995, updated 1995, updated 2016) are used to compare the overall frequency of observed icebergs between 40°N–65°N and 39°W–57°W. The northernmost limit was increased from 52°N to 65°N after 2006, when the IIP joined efforts with the CIS. The data are obtained by direct sightings from vessels and aircraft, as well as by buoys, radar, and model short-term forecast. Here we only consider observed icebergs with medium to very large sizes, since those are in the same range as the ones represented by the model.

3. Results

Figure 2 shows the number of particles that crossed each grid point throughout the simulation, providing a general display of Greenland icebergs distribution. The icebergs in *VERT* (Figure 2b) tend to follow—or be restrained by—the main ocean currents indicated in Figure 1, which are at least partially resolved by the grid resolution (~15 km around Greenland; see Figure S2 for average speed in the simulations). The Transpolar

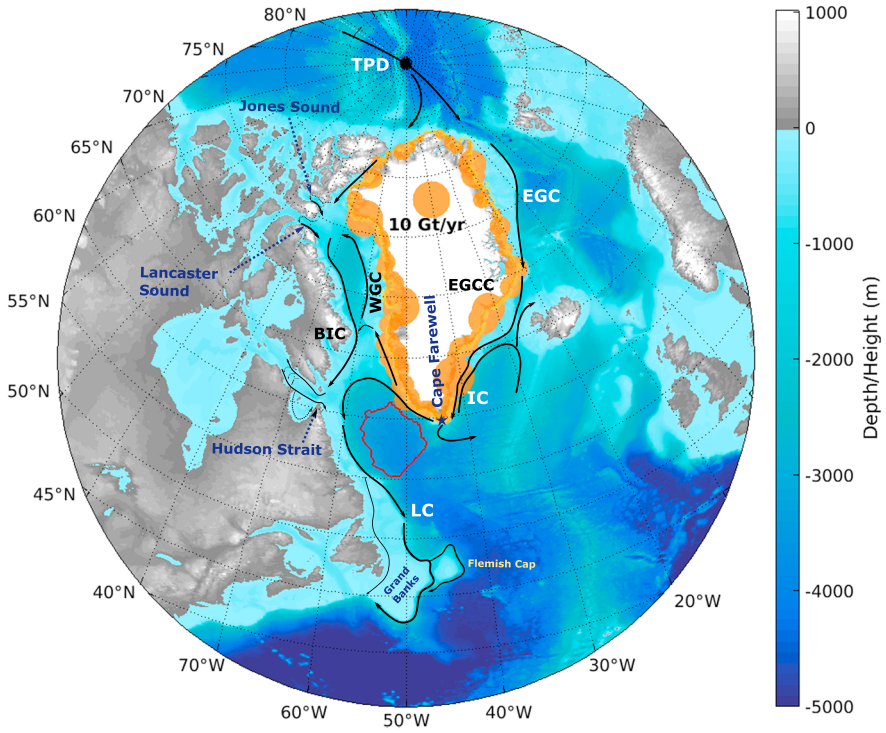


Figure 1. Map showing the main currents affecting Greenland icebergs drift: Transpolar Drift (TPD), East Greenland Current (EGC), East Greenland Coastal Current (EGCC), Irminger Current (IC), West Greenland Current (WGC), Baffin Island Current (BIC), and Labrador Current (LC). The orange circles represent average calving rates (2002–2010), in Gt/year, seeded to the iceberg model on the ANHA4 grid. The rates correspond to 54% of the total mass loss estimated by Bamber et al. (2012). The red contour delineates the interior Labrador Sea (3,000 m isobath).

Drift, for example, which heads toward North Greenland, prevents icebergs from this region further spreading into Arctic's interior. Along Greenland's east coast, icebergs follow the East Greenland Coastal Current (EGCC), East Greenland Current (EGC), and the Irminger Current (e.g., Sutherland & Pickart, 2008). Particles that reach Cape Farewell may recirculate eastward (Holliday et al., 2007, 2009), separate from the west coast at ~63°N and enter the Labrador Sea or continue with the northward branch of the West Greenland Current (WGC). The last two pathways are consistent with the trajectories observed by Marko et al. (1982, 1994). Icebergs also concentrate along the Baffin Island Current and, finally, join the Labrador Current (LC) on their way to the Grand Banks. Figure 2b also shows icebergs entering Hudson Strait and the Canadian Arctic Archipelago (CAA) through Jones Sound and Lancaster Sound, where icebergs are known to threaten observational systems (Hamilton & Pittman, 2015).

While the icebergs in *VERT* (Figure 2b) are prone to move along the shelf break, icebergs in *SURF* (Figure 2a) concentrate near the coastline (difference in Figure 2c). Both simulations have less than 10 particles per grid cell crossing the distribution limit considered "normal" by the IIP (dashed red lines in Figures 2a and 2b). In the area monitored by the IIP (Figures 2g and 2h), icebergs in *VERT* preferentially follow a branch of the LC that goes around Flemish Cap (Stein, 2007), while in *SURF* they tend to be carried by the LC inshore branch or go through the Flemish Pass (see branches in Figure 1). Figure 2i shows that the pattern drawn by the IIP-observed icebergs in the same period (2002–2015) resembles more that of the *SURF* simulation. The seasonal cycle of icebergs crossing 48°N (Figure 2j) is better constrained in *VERT* where the iceberg season happens between March and July as in the observations (Wilton et al., 2015), while in *SURF* it starts in December. The difference between *VERT* and observed seasonal cycles is that the former has a double-peak shape (in March and May), while the latter only peaks in May.

Figures 3a and 3b show the average lifetime of icebergs passing through each grid cell in *SURF* and *VERT*, respectively. In general, modeled icebergs tend to melt faster in the interior of the Labrador Sea, Irminger Sea, and southern sectors of Greenland coast (lifetime restricted to about 6 months). Lasting 12 to 18 months are the icebergs between east Greenland and Iceland, icebergs that stay north of Baffin Bay and along the Baffin

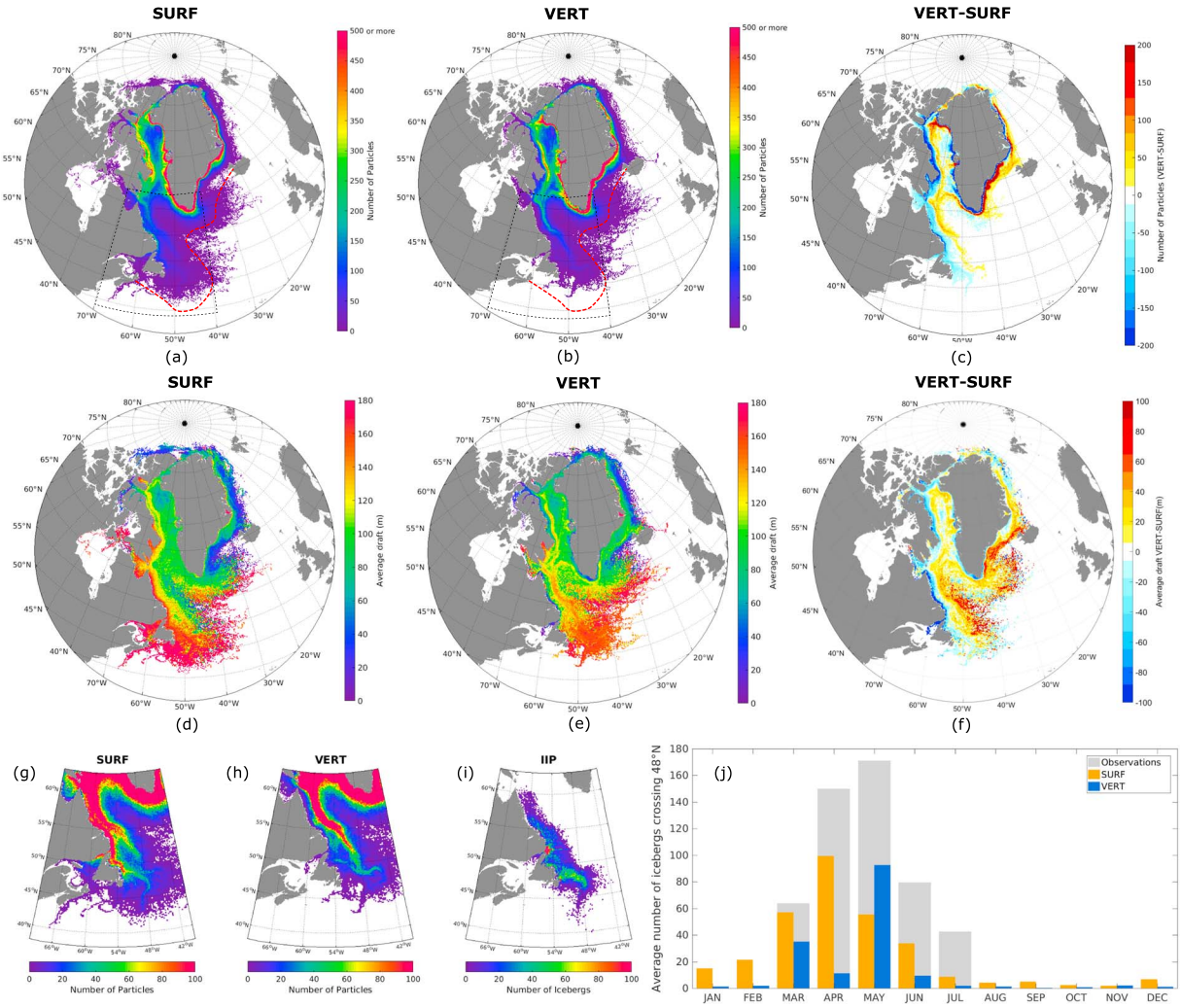


Figure 2. Total number of particles that passed through each grid point between 2002 and 2015 in (a) *SURF* and (b) *VERT*. The dashed red line marks the normal range of icebergs determined by the International Ice Patrol (IIP), and the dashed black lines indicate the location of (g) and (h). The difference between (b) and (a) is shown in (c). Average iceberg draft is shown in (d) for *SURF*, (e) for *VERT*, and (f) shows their difference. Panels (g) and (h) are details for the IIP-monitored region from (a) and (b) respectively. (i) Number of icebergs counted by the IIP between 2002 and 2015 and (j) monthly average of the number of icebergs crossing 48°N between 2010 and 2015 for the IIP (grey), *SURF* (orange), and *VERT* (blue).

Island coast, and icebergs that reach the Grand Banks via LC. Icebergs that enter Hudson Strait and the CAA tend to live for two or more years. The oldest icebergs are found in the Arctic and are consistently calved from the northern Greenland sector, as will be seen in Figure 4. Icebergs in *VERT* melt completely 112 days earlier than in *SURF*, on average. Regionally, *VERT* icebergs last significantly less (by one year or more) in the NE sector of Greenland, and slightly longer (by around 2 months) along the LC (Figure 3c). Beyond the sea ice line, the differences seem to be more random. Figure 3d shows the difference between the integrated temperature along average iceberg draft (~100 m) and surface temperature only. It can be seen that warmer Atlantic waters flow below colder Arctic waters around Greenland, which explains the dominant decrease in lifetime in *VERT* compared to *SURF* (more details in the next section).

To determine the most common origin of icebergs in a certain region, we divided the Greenland coast into five sectors (Figure 4, middle). The percentage of icebergs that came from each sector (calculated at each grid point) in *VERT* is shown in Figure 4. Icebergs that calve from Greenland's north sector often remain near their origin and within the EGC in the Nordic Seas (Figure 4a). Particles that originate in the northeast (Figure 4b) make up the majority of those drifting along eastern Greenland, onshoreward from EGC. The EGCC carries southeastern icebergs, most of which will be advected to the Irminger Sea by the recirculation at Cape Farewell (Holliday et al., 2007, 2009) or enter the Labrador Sea interior (Figure 4c). The icebergs calved from the east

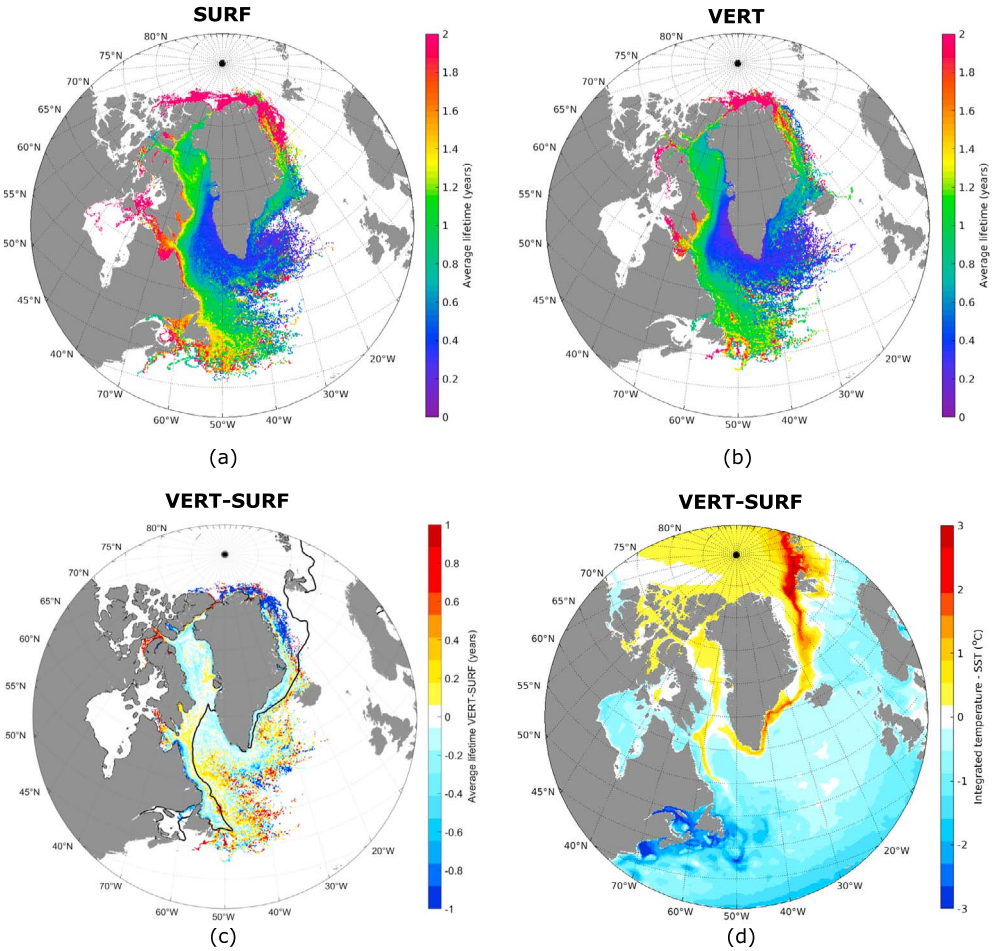


Figure 3. Average lifetime per grid cell between 2002 and 2015 in (a) *SURF* and (b) *VERT*. The difference in lifetime (*VERT-SURF*) is depicted in (c), where the black line marks the March-averaged sea ice edge (sea ice concentration of 15%) in *VERT*; panel (d) shows the difference between integrated temperatures from surface to ~100 m from *VERT* and sea surface temperature from *SURF*.

sectors rarely enter Baffin Bay; instead of following the northward branch of WGC, they separate from the coast and join the LC in its southward journey. This pattern agrees with previous findings that most part of WGC turns westward before it reaches Davis Strait (e.g., Fratantoni & Pickart, 2007). Icebergs calved from the southwest sector (Figure 4d) are more locally dominant because the number of particles calved from this sector is considerably smaller than the number produced by the southeast and northwest coasts (ratios of 1:1.6 and 1:1.4, respectively). Nevertheless, southwestern icebergs may follow Baffin Bay's cyclonic circulation before joining the LC or, more commonly, cross south of Davis Strait to travel along the Labrador Sea shelf break and reach the Grand Banks. Finally, the northwest sector is the dominant source of icebergs that populate Baffin Bay, enter Hudson Strait and the CAA through its eastern passages, and drift with the LC south to reach the Grand Banks and spread east with the North Atlantic Current (Figure 4e). The dominance of NW icebergs crossing 48°N was shown to be characteristic from the period post-1930 (Wilton et al., 2015).

4. Discussion

Although the iceberg momentum balance equation (shown in Text S1) involves different terms that have distinct importance regionally and temporally (Bigg et al., 1997), the fundamental difference between the *SURF* and *VERT* iceberg distribution (Figures 2a and 2b) occurs in the ocean drag term. This term is dependent on ocean velocity, which is given either by the surface velocity in *SURF* or by an integration from surface to iceberg keel in *VERT*. Therefore, the differences shown in Figure 2c happen mainly due to the different circulation regimes at surface and subsurface, which affect the trajectory of icebergs with drafts larger than ~100 m

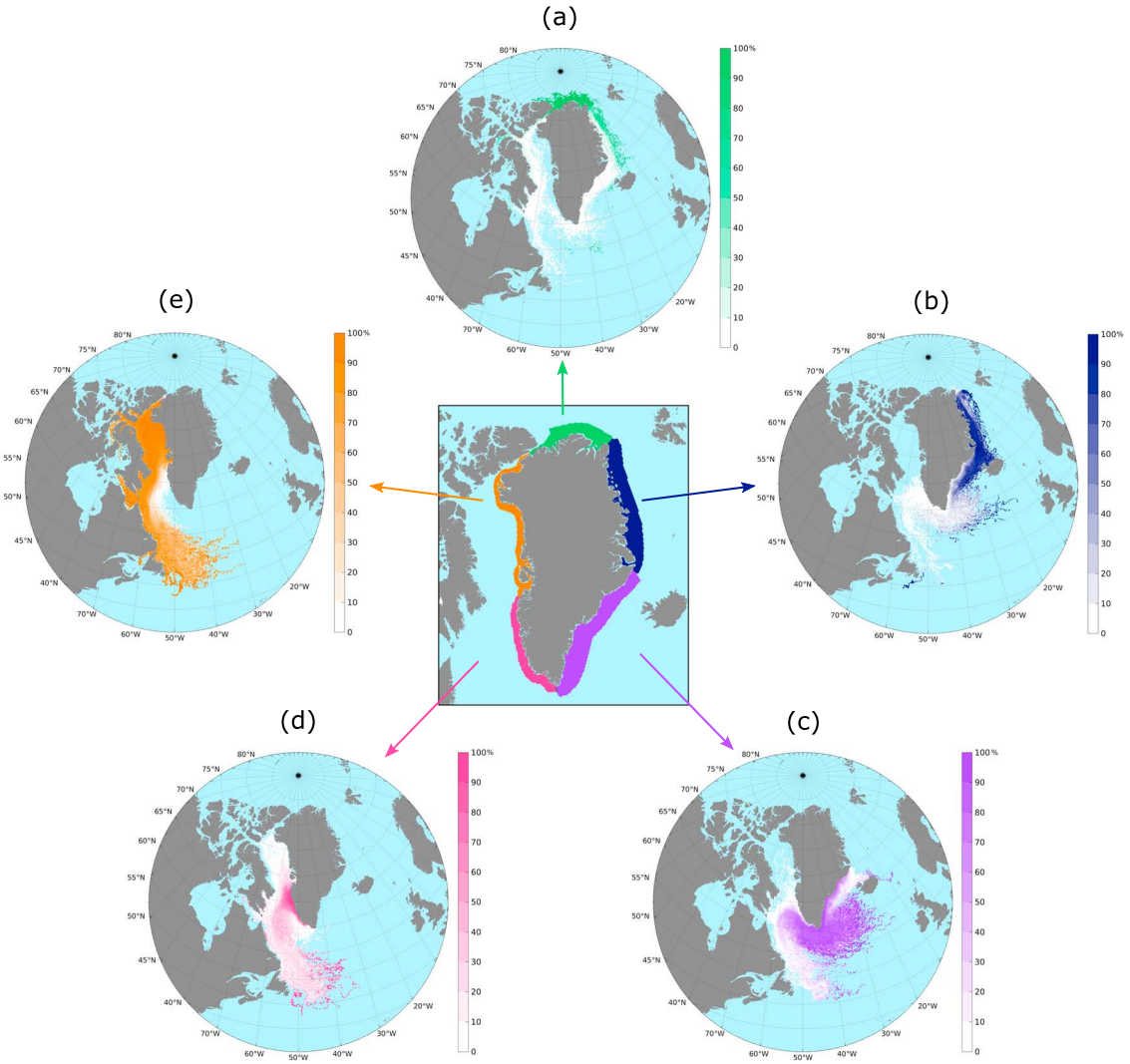


Figure 4. Origin of icebergs in *VERT* (2002–2015). The intensity of colors indicates, at each grid point, the percentage of particles that came from (a) north, (b) northeast, (c) southeast, (d) southwest, and (e) northwest.

(Figures 2d and 2e). When using only the surface velocity field, icebergs are primarily driven by Ekman drift, which points toward the coastline in Baffin Bay and Labrador Sea due to the characteristic low-pressure systems over these regions. Figure 2d shows that this tendency is even more pronounced for larger icebergs, since those are more affected by the drag from the ocean rather than the atmosphere (the ocean drag term is dependent on iceberg draft and length; Text S1). On the other hand, by integrating the velocity field along iceberg drafts over ~100 m (deeper than the typical Ekman depth), the importance of the geostrophic flow increases. Since geostrophic currents are approximately in the same direction as predominant winds, which blow away from the coast (e.g., Tang et al., 2004), icebergs with drafts larger than 100 m are pushed offshoreward (Figure 2e). The concentration of icebergs along the Baffin Island shelf break was pointed out by Robe et al. (1980) and Marko et al. (1982) using buoys and satellite-tracked iceberg data. Therefore, the *VERT* simulation seems to reproduce better the icebergs distribution in this region. The difference in iceberg distribution between *VERT* and *SURF* also causes the icebergs to melt in different regions, resulting in surface salinity anomalies up to ~0.2 along Greenland coast (see Figure S1). As expected, icebergs move slower in *VERT* (average speed of 0.19 m/s) than in *SURF* (average speed of 0.23 m/s) due to current shear with depth (see Figure S2), which will impact their lifetime.

When comparing the simulated iceberg distributions with observations in the area monitored by the IIP, Figure 2i showed more resemblance with *SURF*. Although the number of observations may be biased

toward the coast, within the range of reconnaissance flights and ship lanes, we need to consider that the physics in the iceberg model might still be too simplified to capture iceberg distribution south of 55° N. Reasons that may lead to such inconsistencies between the *VERT* simulation and observations are listed below:

1. There is no sea ice locking of icebergs when sea ice is thick and compact. This is important both in permanently covered regions (such as north of Greenland), where keeping icebergs longer leads to increasing iceberg lifetime due to sea ice damping effect on waves, and in seasonally covered regions such as Baffin Bay, where the seasonal freezing and melting of sea ice controls the timing of icebergs that reach the Grand Banks (Marko et al., 1994). Marsh et al. (2018) showed that variations in this timing may cause icebergs to move more onshore or offshoreward. Introducing sea ice locking could, therefore, fix the double-peak seasonal cycle in *VERT* and, consequently, change the icebergs' average distance from the coast.
2. Icebergs only slow down in shallow regions instead of being completely grounded. Proper grounding of icebergs would allow them to reduce their draft before reaching this far south, which then would cause icebergs to be more affected by surface currents rather than geostrophic ones. Surface currents would then, through Ekman transport, push these relatively small icebergs toward the inshore branch of the LC (Figure 2e, icebergs with smaller drafts concentrate over the shelf).
3. All icebergs are block shaped, which may lead to an overestimated keel area, not only because other shapes imply a different freeboard:draft ratio but also because icebergs tend to be narrower toward its bottom (Barker et al., 2004), which would reduce the area over which ocean drag can act.
4. The resolution used does not allow the representation of fjords, where icebergs lose about 50% of their initial mass before entering open ocean (Enderlin et al., 2016) and may be trapped in the ice mélange before the melting season (e.g., Vaňková & Holland, 2017), altering the timing of icebergs that would reach the Grand Banks.

Icebergs' lifetime was studied before with models, and it is often associated with their size. Bigg et al. (1997) pointed out that in their simulations, the smallest icebergs (60 m length) melted completely within 1 year. Bügelmayer et al. (2015) also reported that modeled icebergs from 67 to 200 m melted completely within 2 years. However, Figures 2d and 2e show that the spatial distribution of iceberg's average draft (proportional to their size) is significantly different from the lifetime maps in Figures 3a and 3b. In fact, the icebergs that lived longer in our simulation (over 13 years in *VERT*) have lengths around 200 m—the third smallest iceberg class in the simulation (see Table S1 for iceberg classes and sizes). While the iceberg mass balance equation indeed depends on the iceberg dimensions (see Text S1), it also depends on turbulence at the base of the iceberg, sea state, and ocean temperature, and their importance to lifetime varies depending on the region the icebergs live (see those relationships in Figure S3). Here the longevity is usually associated with the presence of sea ice, which reduces iceberg deterioration due to (i) its damping effect on wave energy (Gladstone et al., 2001)—thus reducing wave erosion, the most efficient mechanism of iceberg deterioration in the simulation—and (ii) its associated temperatures below 0°C. Therefore, icebergs last more than 2 years in areas where sea ice is present most of the year (northern sector) while lasting around 1 year in areas seasonally covered by sea ice (delimited by black line in Figure 3c). On the other hand, the ones that pass through ice-free regions influenced by the advection of warmer waters (blue areas in Figure 3b) have a lifetime on the order of months. In those regions, the size of the icebergs becomes more important: icebergs that travel progressively southward are increasingly larger (Figure 2e).

When we compare lifetime changes between the two simulations (Figure 3c), the overall reduction in *VERT* is primarily associated to the ocean temperature used in the mass balance equation: as predicted by Marsh et al. (2015), the inclusion of warm Atlantic subsurface waters in the temperature average used to melt icebergs reduced their lifetime significantly where this water mass is present—especially off NE Greenland, where Atlantic water enters the Arctic through Fram Strait (Figure 3d). The slight increase in lifetime along the LC in Figure 3c seems, however, unrelated to how the temperature for iceberg melt is calculated, since warmer-than-surface waters are present there as well. This increase might be explained simply because the icebergs present in this region in *VERT* are larger than in *SURF* (see Figures 2d–2f), or might be associated with the slower speeds icebergs have along west boundaries in *VERT* (Figure S2c), allowing them to remain in cold waters longer and delaying their complete melting. The differences in areas usually not covered by sea ice (delimited by the black line in Figure 3c) are random and possibly associated to different iceberg sizes.

In addition to the four shortcomings in *VERT* mentioned before, other limitations that may affect the number of icebergs and their lifetime in the simulations are listed below:

5. There is no latent heat flux between icebergs and ocean, which would cool surface waters near the icebergs and delay their melting.
6. We have not included bergy bits resulting from iceberg break up due to wave erosion. Bergy bits also tend to prolong the icebergs lifetime (Martin & Adcroft, 2010).
7. The ratio between liquid and solid discharge is not the same for every glacier, so our simulation can be under or overestimating calving rates in certain regions.

Almost 60% of the icebergs crossing the 3,000 m isobath in the Labrador Sea (red contour in Figure 1) originate from the SE sector (Figure 4c). The remaining 40% are split between the icebergs calved from other sectors: SW (16%), NW (16%), NE (7%), and N (1%). Gillard et al. (2016), while studying the fate of Greenland *liquid* discharge from the same five sectors, found that ~80% of Greenland melt that entered the Labrador Sea 3,000 m isobath originated from the SE sector. Although the relative solid discharge contribution from SE is smaller than the liquid one, the dominance of the SE sector as a source of freshwater in all its forms to the interior Labrador Sea indicates that further increases in discharge from this sector could impact Labrador Sea deep convection. Böning et al. (2016) pointed out that although Greenland meltwater has been negligible compared to the strong freshwater variability in the Labrador Sea, an interruption of deep convection can be expected by 2040 if current GrIS discharge rates are maintained or increased.

5. Summary and Conclusions

Previous studies have showed that icebergs are mainly driven by current speed and direction (Allison et al., 2014; Bigg et al., 1996). Nevertheless, the fact that icebergs may extend for hundreds of meters down the water column and so are likely to have their trajectories affected by current shear and direction change beyond the Ekman layer has been dismissed in most iceberg models, which use only surface ocean fields to calculate their drift and deterioration. As pointed out by FitzMaurice et al. (2016), who observed around 90 icebergs in SE Greenland, those models can have errors of 60% or more when estimating iceberg speed and basal melt in strongly sheared flows. In this study, we have used an iceberg model that integrates the ocean fields from surface to iceberg keel before using them in the iceberg's dynamic and thermodynamic equations (Merino et al., 2016), here applied to the Northern Hemisphere for the first time. Compared to the previous surface-driven iceberg model (*SURF*), the vertically integrated version (*VERT*) better reproduced the concentration of Greenland icebergs within the main ocean currents, which in general occur along the shelf break. The icebergs' lifetime in *VERT* was also altered from *SURF*, since it allows warm subsurface waters to melt medium-to-large icebergs faster. Additionally, we have pointed out that the presence of sea ice damps waves and therefore reduces their importance on iceberg deterioration, allowing icebergs to survive longer regardless of their initial size.

We have also shown that icebergs calving from different sectors of Greenland tend to populate different areas. Icebergs calved from the north and southwest sectors are more commonly found offshoreward of EGC and LC, respectively, while northeastern and northwestern icebergs are preferentially located onshoreward of these same currents. Moreover, while icebergs that calved from the west coast tend to enter Baffin Bay and then drift southward with the LC, eastern icebergs rarely do so. Particularly, the southeast sector is the main source of icebergs (~60%) that cross the interior of the Labrador Sea — the same behavior that was found for Greenland's liquid freshwater pathways (Gillard et al., 2016; Luo et al., 2016). These icebergs deserve a closer look, since a potential increase in the calving rates of southeastern glaciers could affect deep convection in the Labrador Sea (Böning et al., 2016).

We highlight that although *VERT* represents better the larger iceberg trajectories within geostrophic currents, it is still missing or oversimplifying important physical parameterizations that may be detrimental to reproduce icebergs observed south of 55°N. Among them, the absence of bergy bits and latent heat flux was fixed in our newest configuration. Sea ice locking, which was implemented in the Finite Element Sea ice-Ocean Model by Rackow et al. (2017), is currently being adapted to NEMO. We also have converted part of the solid discharge into liquid before calving icebergs to simulate the mass loss of icebergs inside fjords, following estimates by Enderlin et al. (2016) and Moon et al. (2018). Calving rates estimates were improved with the updated data set from Bamber et al. (2018), where solid discharge is given as a separate variable

(instead of being estimated by multiplying total Greenland discharge by 54% as described in section 2). Our next step is to evaluate the impact of iceberg heat and freshwater flux to sea ice cover, stratification, and subduction in the Labrador Sea.

Acknowledgments
For access to the model output, visit http://knossos.eas.ualberta.ca/xianmin/anha/anhatable.html. We gratefully acknowledge the financial and logistic support of grants from the Natural Sciences and Engineering Research Council of Canada (RGPIN 04357 and RGPCC 433898) and Polar Knowledge Canada (PKC-NST-1617-0003). We are grateful to the NEMO development team and the Drakkar project for providing the model and continuous guidance and to Westgrid and Compute Canada for computational resources. We would also like to thank G. Smith for the CGRF forcing fields, made available by Environment and Climate Change Canada, and G. Garric for the GLORYS2v3 output. Greenland freshwater flux data analyzed in this study is that presented in Bamber et al. (2012) and is available on request as a gridded product. We also thank Nacho Merino, who shared his vertically integrated version of the iceberg model with us and offered some valuable insights. To the reviewers, we appreciate your suggestions which greatly improved the final version of this paper.

References

Allison, K., Crocker, G., Tran, H., & Carrieres, T. (2014). An ensemble forecast model of iceberg drift. *Cold Regions Science and Technology*, *108*, 1–9. https://doi.org/10.1016/j.coldregions.2014.08.007

Bamber, J. L., Tedstone, A. J., King, M. D., Howat, I. M., Enderlin, E. M., van den Broeke, M. R., & Noel, B. (2018). Land ice freshwater budget of the Arctic and North Atlantic Oceans: 1. Data, Methods, and Results. *Journal of Geophysical Research: Oceans*, *123*, 1827–1837. https://doi.org/10.1002/2017JC013605

Bamber, J., van den Broeke, M., Ettema, J., Lenaerts, J., & Rignot, E. (2012). Recent large increases in freshwater fluxes from Greenland into the North Atlantic. *Geophysical Research Letters*, *39*, L19501. https://doi.org/10.1029/2012GL052552

Barker, A., Sayed, M., & Carrieres, T. (2004). Determination of iceberg draft, mass and cross-sectional areas. In *Proceedings of the Fourteenth (2004) International Offshore and Polar Engineering Conference* (pp. 899–904). Toulon, France.

Bigg, G. R. (1999). An estimate of the flux of iceberg calving from Greenland. *Arctic, Antarctic, and Alpine Research*, *31*(2), 174–178.

Bigg, G. R., Wadley, M. R., Stevens, D. P., & Johnson, J. A. (1996). Prediction of iceberg trajectories for the North Atlantic and Arctic oceans. *Geophysical Research Letters*, *23*(24), 3587–3590. https://doi.org/10.1029/96GL03369

Bigg, G. R., Wadley, M. R., Stevens, D. P., & Johnson, J. A. (1997). Modelling the dynamics and thermodynamics of icebergs. *Cold Regions Science and Technology*, *26*(2), 113–135. https://doi.org/10.1016/S0165-232X(97) 00012-8

Böning, C. W., Behrens, E., Biastoch, A., Getzlaff, K., & Bamber, J. L. (2016). Emerging impact of Greenland meltwater on deepwater formation in the North Atlantic Ocean. *Nature Geoscience*, *9*, 523–527. https://doi.org/10.1038/ngeo2740

Bouillon, S., Morales Maqueda, M., Legat, V., & Fichefet, T. (2009). An elastic-viscous-plastic sea ice model formulated on Arakawa B and C grids. *Ocean Modelling*, *27*, 174–184. https://doi.org/10.1016/j.ocemod.2009.01.004

Bügelmayer, M., Roche, D. M., & Renssen, H. (2015). Representing icebergs in the iLOVECLIM model (version 1.0)—A sensitivity study. *Geoscientific Model Development*, *8*(7), 2139–2151. https://doi.org/10.5194/gmd-8-2139-2015

Dukhovskoy, D. S., Myers, P. G., Platov, G., Timmermans, M.-L., Curry, B., Proshutinsky, A., et al. (2016). Greenland freshwater pathways in the sub-Arctic Seas from model experiments with passive tracers. *Journal of Geophysical Research: Oceans*, *121*, 877–907. https://doi.org/10.1002/2015JC011290

Duprat, L. P. A. M., Bigg, G. R., & Wilton, D. J. (2016). Enhanced Southern Ocean marine productivity due to fertilization by giant icebergs. *Nature Geoscience*, *9*(3), 219–221. https://doi.org/10.1038/ngeo2633

Enderlin, E. M., Hamilton, G. S., Straneo, F., & Sutherland, D. A. (2016). Iceberg meltwater fluxes dominate the freshwater budget in Greenland's iceberg-congested glacial fjords. *Geophysical Research Letters*, *43*, 11,287–11,294. https://doi.org/10.1002/2016GL070718

Enderlin, E. M., Howat, I. M., Jeong, S., Noh, M.-J., van Angelen, J. H., & van den Broeke, M. R. (2014). An improved mass budget for the Greenland ice sheet. *Geophysical Research Letters*, *41*, 866–872. https://doi.org/10.1002/2013GL059010

Fichefet, T., & Morales Maqueda, M. (1997). Sensitivity of a global sea ice model to the treatment of ice thermodynamics and dynamics. *Journal of Geophysical Research*, *102*, 12,609–12,646. https://doi.org/10.1029/97JC00480

FitzMaurice, A., Straneo, F., Cenedese, C., & Andres, M. (2016). Effect of a sheared flow on iceberg motion and melting. *Geophysical Research Letters*, *43*, 12,520–12,527. https://doi.org/10.1002/2016GL071602

Fratantoni, P. S., & Pickart, R. S. (2007). The western North Atlantic shelfbreak current system in summer. *Journal of Physical Oceanography*, *37*(10), 2509–2533. https://doi.org/10.1175/jpo3123.1

Gillard, L. C., Hu, X., Myers, P. G., & Bamber, J. L. (2016). Meltwater pathways from marine terminating glaciers of the Greenland ice sheet. *Geophysical Research Letters*, *43*, 10,873–10,882. https://doi.org/10.1002/2016GL070969

Gladstone, R. M., Bigg, G. R., & Nicholls, K. W. (2001). Iceberg trajectory modeling and meltwater injection in the Southern Ocean. *Journal of Geophysical Research*, *106*(C9), 19,903–19,915. https://doi.org/10.1029/2000JC000347

Hamilton, J. M., & Pittman, M. D. (2015). Sea-ice freeze-up forecasts with an operational ocean observatory. *Atmosphere-Ocean*, *53*(5), 595–601. https://doi.org/10.1080/07055900.2014.1002447

Holliday, N. P., Bacon, S., Allen, J., & McDonagh, E. L. (2009). Circulation and transport in the western boundary currents at Cape Farewell, Greenland. *Journal of Physical Oceanography*, *39*(8), 1854–1870. https://doi.org/10.1175/2009JPO4160.1

Holliday, N. P., Meyer, A., Bacon, S., Alderson, S. G., & de Cuevas, B. (2007). Retroflection of part of the east Greenland current at Cape Farewell. *Geophysical Research Letters*, *34*, L07609. https://doi.org/10.1029/2006GL029085

International Ice Patrol (1995, updated 2016). International Ice Patrol (IIP) iceberg sightings database, version 1, NSIDC: National Snow and Ice Data Center, Boulder, Colorado, USA. https://doi.org/10.7265/N56Q1V5R

Luo, H., Castelao, R. M., Rennermalm, A. K., Tedesco, M., Bracco, A., Yager, P. L., & Mote, T. L. (2016). Oceanic transport of surface meltwater from the southern Greenland ice sheet. *Nature Geoscience*, *9*(7), 528–532. https://doi.org/10.1038/ngeo2708

Madec, G., & the NEMO team (2008). NEMO ocean engine, Note du Pole de modelisation, Institut Pierre-Simon Laplace (IPSL), France, 27. ISSN 1288–1619.

Marko, J. R., Birch, J. R., & Wilson, M. A. (1982). A study of long-term satellite-tracked iceberg drifts in Baffin Bay and Davis Strait. *Arctic*, *35*(1), 234–240.

Marko, S. R., Fissel, D. B., Wadhams, P., Kelly, P. M., & Brown, R. D. (1994). Iceberg severity of eastern North America: Its relationship to sea ice variability and climate change. *Journal of Climate*, *7*(9), 1335–1351.

Marsh, R., Bigg, G., Zhao, Y., Martin, M. J., Blundell, J. R., Josey, S. A., et al. (2018). Prospects for seasonal forecasting of iceberg distributions in the North Atlantic. *Natural Hazards*, *91*(2), 447–471. https://doi.org/10.1007/s11069-017-3136-4

Marsh, R., Ivchenko, V. O., Skliris, N., Alderson, S., Bigg, G. R., Madec, G., et al. (2015). NEMO-ICB (v1.0): Interactive icebergs in the NEMO ocean model globally configured at eddy-permitting resolution. *Geoscientific Model Development*, *8*(5), 1547–1562. https://doi.org/10.5194/gmd-8-1547-2015

Martin, T., & Adcroft, A. (2010). Parameterizing the fresh-water flux from land ice to ocean with interactive icebergs in a coupled climate model. *Ocean Modelling*, *34*(3-4), 111–124. https://doi.org/10.1016/j.ocemod.2010.05.001

Masina, S., Storto, A., Ferry, N., Valdivieso, M., Haines, K., Balmaseda, M., et al. (2015). An ensemble of eddy-permitting global ocean reanalyses from the MyOcean project. *Climate Dynamics*, *49*, 813–841. https://doi.org/10.1007/s00382-015-2728-5

Merino, N., Sommer, J. L., Durand, G., Jourdain, N. C., Madec, G., Mathiot, P., & Tournadre, J. (2016). Antarctic icebergs melt over the Southern Ocean: Climatology and impact on sea ice. *Ocean Modelling*, *104*, 99–110. https://doi.org/10.1016/j.ocemod.2016.05.001

Moon, T., Sutherland, D. A., Carroll, D., Felikson, D., Kehrl, L., & Straneo, F. (2018). Subsurface iceberg melt key to Greenland fjord freshwater budget. *Nature Geoscience*, *11*(1), 49–54. https://doi.org/10.1038/s41561-017-0018-z

Pizzolato, L., Howell, S. E. L., Dawson, J., Laliberté, F., & Copland, L. (2016). The influence of declining sea ice on shipping activity in the Canadian Arctic. *Geophysical Research Letters*, *43*, 12,146–12,154. https://doi.org/10.1002/2016GL071489

Rackow, T., Wesche, C., Timmermann, R., Hellmer, H. H., Juricke, S., & Jung, T. (2017). A simulation of small to giant Antarctic iceberg evolution: Differential impact on climatology estimates. *Journal of Geophysical Research: Oceans*, *122*, 3170–3190. https://doi.org/10.1002/2016JC012513

Rignot, E., Velicogna, I., van den Broeke, M. R., Monaghan, A., & Lenaerts, J. T. M. (2011). Acceleration of the contribution of the Greenland and Antarctic ice sheets to sea level rise. *Geophysical Research Letters*, *38*, L05503. https://doi.org/10.1029/2011GL046583

Robe, R., Maier, D., & Russell, W. (1980). Long-term drift of icebergs in Baffin Bay and the Labrador Sea. *Cold Regions Science and Technology*, *1*(3), 183–193. https://doi.org/10.1016/0165-232X(80)90047-6

Smith, G. C., Roy, F., Mann, P., Dupont, F., Brasnett, B., Lemieux, J.-F., et al. (2014). A new atmospheric dataset for forcing ice-ocean models: Evaluation of reforecasts using the Canadian global deterministic prediction system. *Quarterly Journal of the Royal Meteorological Society*, *140*(680), 881–894. https://doi.org/10.1002/qj.2194

Stein, M. (2007). Oceanography of the Flemish Cap and adjacent waters. *Journal of Northwest Atlantic Fishery Science*, *37*, 135–146. https://doi.org/10.2960/J.v37.m652

Straneo, F., Heimbach, P., Sergienko, O., Hamilton, G., Catania, G., Griffies, S., et al. (2013). Challenges to understanding the dynamic response of Greenland's marine terminating glaciers to oceanic and atmospheric forcing. *Bulletin of the American Meteorological Society*, *94*(8), 1131–1144. https://doi.org/10.1175/BAMS-D-12-00100.1

Stroeve, J. C., Kattsov, V., Barrett, A., Serreze, M., Pavlova, T., Holland, M., & Meier, W. N. (2012). Trends in Arctic sea ice extent from CMIP5, CMIP3 and observations. *Geophysical Research Letters*, *39*, L16502. https://doi.org/10.1029/2012GL052676

Sutherland, D. A., & Pickart, R. S. (2008). The East Greenland Coastal Current: Structure, variability, and forcing. *Progress in Oceanography*, *78*(1), 58–77. https://doi.org/10.1016/j.pocean.2007.09.006

Tang, C. C., Ross, C. K., Yao, T., Petrie, B., DeTracey, B. M., & Dunlap, E. (2004). The circulation, water masses and sea-ice of Baffin Bay. *Progress in Oceanography*, *63*(4), 183–228. https://doi.org/10.1016/j.pocean.2004.09.005

Tournadre, J., Whitmer, K., & Girard-Ardhuin, F. (2008). Iceberg detection in open water by altimeter waveform analysis. *Journal of Geophysical Research*, *113*, C08040. https://doi.org/10.1029/2007JC004587

Vaňková, I., & Holland, D. M. (2017). A model of icebergs and sea ice in a joint continuum framework. *Journal of Geophysical Research: Oceans*, *122*, 9110–9125. https://doi.org/10.1002/2017JC013012

Wesche, C., & Dierking, W. (2012). Iceberg signatures and detection in SAR images in two test regions of the Weddell Sea, Antarctica. *Journal of Glaciology*, *58*(208), 325–339. https://doi.org/10.3189/2012J0G11J020

Wesche, C., & Dierking, W. (2015). Near-coastal circum-Antarctic iceberg size distributions determined from Synthetic Aperture Radar images. *Remote Sensing of Environment*, *156*, 561–569. https://doi.org/10.1016/j.rse.2014.10.025

Wilton, D. J., Bigg, G. R., & Hanna, E. (2015). Modelling twentieth century global ocean circulation and iceberg flux at 48N: Implications for west Greenland iceberg discharge. *Progress in Oceanography*, *138*, 194–210. https://doi.org/10.1016/j.pocean.2015.07.003